

## Field-induced soft mode hardening in SrTiO<sub>3</sub>/DyScO<sub>3</sub> multilayers

P. Kužel,<sup>1,a)</sup> C. Kadlec,<sup>1</sup> F. Kadlec,<sup>1</sup> J. Schubert,<sup>2</sup> and G. Panaitov<sup>2</sup>

<sup>1</sup>*Institute of Physics, Academy of Sciences of the Czech Republic, Na Slovance 2, 182 21 Prague 8, Czech Republic*

<sup>2</sup>*Institute of Bio- and Nanosystems and Center of Nanoelectronics and Information Technology (CNI), Forschungszentrum Jülich, GmbH, D 52425, Germany*

(Received 27 March 2008; accepted 15 July 2008; published online 7 August 2008)

We investigate a SrTiO<sub>3</sub>/DyScO<sub>3</sub> epitaxial multilayer with four 50-nm-thick layers of each compound deposited on DyScO<sub>3</sub> substrate by pulsed laser deposition. The spectra of SrTiO<sub>3</sub> obtained using time-domain terahertz spectroscopy at room temperature with and without electrical bias are explained by the ferroelectric soft mode coupled to a silent central peak, where the bare soft mode frequency is the only field-dependent parameter. We show that terahertz and subterahertz properties of the layers are determined solely by a tremendous hardening of the soft mode with increasing field. We demonstrate that our structure induces more than 40% modulation of the transmitted terahertz power in a broad frequency range of 0.65–1.15 THz at 140 V (93 kV/cm) bias. © 2008 American Institute of Physics. [DOI: 10.1063/1.2967336]

Thin film structures based on SrTiO<sub>3</sub> (STO) and/or (Ba,Sr)TiO<sub>3</sub> exhibit a big potential for applications in tunable devices in the gigahertz spectral range.<sup>1</sup> Recently, some works have been published showing promising characteristics of STO thin films for tunable applications also in the terahertz region.<sup>2–4</sup> The dielectric behavior of STO single crystals is fully controlled by the soft mode that exhibits a frequency decrease upon cooling. The contribution of the soft mode to the low-frequency dielectric permittivity is high, owing to its strongly polar character and very low frequency. This leads to an increase in the permittivity of STO and its tunability with decreasing temperature. The electric-field tunability of the dielectric function is related to the strongly anharmonic character of the soft mode.<sup>5,6</sup> The hardening of the soft mode frequency with increasing field has been reported for unstrained STO films.<sup>3,7</sup>

It has been shown that the dielectric properties of STO thin films can be adjusted by strain induced during the epitaxial growth owing to the lattice mismatch between STO and the selected substrate material.<sup>8</sup> STO single crystals remain paraelectric down to the lowest temperatures; however, the ferroelectric phase can be induced and the transition temperature can be increased in the thin films by using substrates inducing tensile strain in the STO layer. STO films grown on a DyScO<sub>3</sub> (DSO) substrate have been extensively studied<sup>9</sup> during the past years because the particular value of the lattice parameter mismatch permits here to shift the ferroelectric transition close to the room temperature, which can be suitable for applications such as tunable filters or terahertz modulators.

In this letter we relate quantitatively the room-temperature tunability of a STO/DSO heterostructure deposited on DSO substrates to the soft mode dynamics and demonstrate the key role of this mode for the tuning even for strained structures.

The experiments were performed using a terahertz time-domain spectroscopy. A special care has been paid to the

sample preparation in order to obtain accurate quantitative results. It is known that the uncertainty in the transmittance phase owing to the terahertz propagation through the substrate can have dramatic effects on the absolute determination of the real part of the permittivity.<sup>10</sup> The error in the refractive index  $\Delta n_f$  of the film due to the phase uncertainty reads  $\Delta n_f d_f \approx n_s \Delta d_s + |d_s - d_r| \Delta n_s$ , where  $\Delta d_s$  is the error in the substrate thickness determination,  $\Delta n_s$  is the uncertainty in its refractive index, and  $d_s$  and  $d_r$  are the thicknesses of the substrate under the thin film and of the reference (bare) substrate, respectively. We have first optically polished two (110)-oriented  $10 \times 10 \times 0.85$  mm<sup>3</sup> DSO substrates to highly plane parallel plates with the same thickness (with 1  $\mu$ m precision). Subsequently we have measured their terahertz refractive index and refined their thickness determination using a method similar to that proposed in Ref. 11. With these precautions we estimate to commit at most a 20% error in the determination of the absolute value of the dielectric function of our STO layers.

Three STO/DSO bilayers with a final STO single layer (where the thickness of each layer was 50 nm, i.e., the total thickness of STO was 200 nm) were epitaxially grown on one of the prepared substrates by pulsed laser deposition, and a  $6 \times 6$  mm<sup>2</sup> interdigitated electrode structure consisting of 5  $\mu$ m wide gold lines and 15  $\mu$ m wide gaps was deposited on top (see Refs. 4 and 12 for further technological details). The electrodes were transparent for the terahertz electric field  $E_{\text{terahertz}} \parallel [101]$ . Note that in contrast to our previous paper<sup>4</sup> the electrodes were deposited in a way to allow measurements with terahertz polarization along the more transparent direction of the DSO substrate; this allows us to access substantially broader spectra. Experiments were made under normal incidence, i.e., the wave vector of the terahertz radiation was parallel to the  $[10\bar{1}]$  direction of the DSO substrate.

For the terahertz time-domain experiments we used a Ti:sapphire femtosecond laser oscillator. Linearly polarized terahertz probing pulses were generated by an interdigitated photoconducting switch<sup>13</sup> and detected using the usual electro-optic sampling scheme with a 1 mm thick  $[110]$  ZnTe crystal.<sup>14</sup> The terahertz field is transverse and probes the in-

<sup>a)</sup>Author to whom correspondence should be addressed. Electronic mail: kuzelp@fzu.cz.

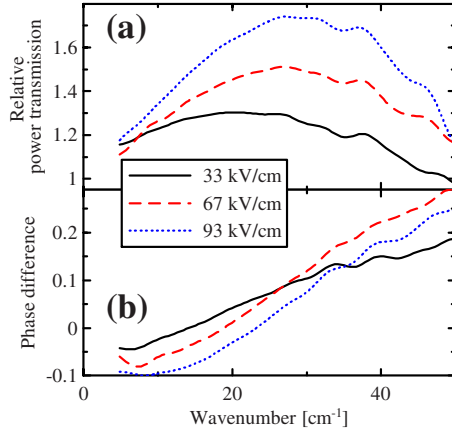


FIG. 1. (Color online) Terahertz transmission spectra of the investigated samples. (a) Ratio of the power transmittances with and without bias. (b) Phase difference between the transmittances with and without bias.

plane complex permittivity  $\varepsilon$  (and refractive index  $n = \varepsilon^{1/2}$ ) of STO layers that are assumed to be homogeneous.<sup>4</sup> The dielectric properties of DSO in the terahertz range are not modified by the applied bias. We followed the procedure described in Ref. 4 for the data acquisition and for the evaluation of the spectra of STO.

The field-induced changes in the terahertz transmission spectra (raw data) are displayed in Fig. 1. The upper panel shows the power transmission spectra of the biased samples normalized to the spectra measured without bias. They exhibit a broad maximum around 30  $\text{cm}^{-1}$  (0.9 THz); in particular, the ratio exceeding 1.65 (corresponding to 40% modulation of the power transmittance) is obtained in the range of 0.64–1.17 THz for the voltage of 140 V (93 kV/cm). This illustrates the figure of merit of these structures for a broadband modulation of terahertz radiation. Figure 1(b) displays the phase difference between the transmission functions of the biased and unbiased samples. The negative phase observed at low frequencies corresponds to a faster terahertz propagation through the STO layers, which is connected to a decrease in their permittivity; the positive phase gives evidence of an increase in its permittivity at high frequencies. This behavior suggests a shift of the resonance in the spectra to higher frequencies with increasing bias. This is indeed observed in the calculated dielectric spectra (Fig. 2).

The evidence of a central mode in the 10–100 GHz range in strained STO structures has been recently obtained,<sup>4,9</sup> and its presence in the spectra close to displacive ferroelectric transition temperatures seems to be a general phenomenon.<sup>15</sup> Therefore we model the measured spectra using a damped oscillator (soft mode with a bare eigenfrequency  $\omega_0$ , damping  $\Gamma$ , and strength  $f$ ) coupled to a Debye relaxation (central mode with a relaxation frequency  $\gamma$ ) by a standard coupled-mode expression<sup>16</sup>

$$\varepsilon(\omega) = S_i S_j G_{ij}(\omega) + \varepsilon_\infty, \quad (1)$$

where  $\varepsilon_\infty$  is the high-frequency permittivity and  $\mathbf{G}(\omega)$  is a Green function matrix of the coupled modes (with a real bilinear coupling constant  $\delta$ )

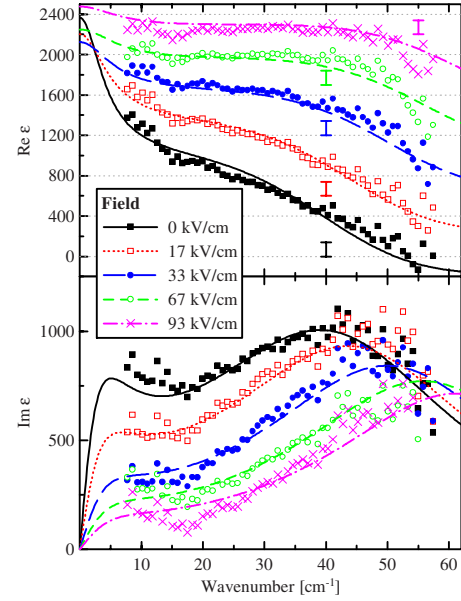


FIG. 2. (Color online) (a) Real and (b) imaginary parts of the permittivity of STO layers for selected external fields; symbols: experiment; lines: fits using Eq. (1). In order to clarify the plot, data corresponding to  $\text{Re } \varepsilon$  were vertically shifted by 400, 800, 1200, and 1600 with increasing field. The vertical bars show the error of our absolute evaluation as deduced from the fitted value of  $\varepsilon_\infty$ .

$$\mathbf{G}^{-1}(\omega) = \begin{pmatrix} 1 - i\omega/\gamma & \delta \\ \delta & \omega_0^2 - \omega^2 - i\omega\Gamma \end{pmatrix}, \quad (2)$$

and the vector  $\mathbf{S} = (0, f^{1/2})$  describes the dielectric strengths of the two modes. This particular form means that the relaxation is assumed to be a silent excitation observable in the spectra only owing to its coupling to the polar soft mode. Figure 2 shows the terahertz spectra for several external fields and their fits with Eq. (1). The hypothesis that the polar dynamics is entirely governed by the soft mode and that the electric-field tuning is due to its anharmonicity directly suggests that the bare soft mode frequency should be the only field-dependent parameter; for small values of the bias E-field it is expected to fulfill the following relation:<sup>6</sup>

$$\omega_0(E) = \omega_0(0) \sqrt{1 + 3\beta[\varepsilon_0 f / \omega_0^2(0)]^3 E^2}, \quad (3)$$

where  $\varepsilon_0$  is the vacuum permittivity and  $\beta$ —the fourth order term in the free energy power expansion<sup>6</sup>—quantifies the anharmonicity of the soft mode potential. In addition, the value of the soft mode oscillator strength  $f \approx 2.3 \times 10^6 \text{ cm}^{-2}$  is known to be valid both for single crystals and thin films and it was kept constant in our fits.

The following values provide the best fits of our data for all values of the field:  $\gamma = 10 \text{ cm}^{-1}$ ,  $\delta = 33 \text{ cm}^{-1}$ , and  $\Gamma = 49 \text{ cm}^{-1}$ . The observed strong damping of the soft mode probably originates from an inhomogeneous broadening due to the gradient of the strain in the layered structure. The coupling constant  $\delta$  is also rather strong making the central mode to appear clearly in the spectra below its bare relaxation frequency  $\gamma$  for low values of the soft mode frequency  $\omega_0$ . This mechanism describes an extra low-frequency decay channel of the ferroelectric mode. Thus the central mode will dominate in the spectra if the soft mode approaches the value of  $\delta$ , i.e., for  $\omega_0 \lesssim 40 \text{ cm}^{-1}$ . Note that even in the case of predominant central mode hiding completely the soft mode peak in its tail, as it was observed, e.g., for the sample 100 A

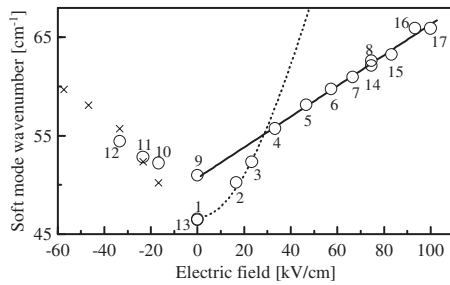


FIG. 3. Soft mode frequency as a function of the external electric field. The numbers indicate the order of individual measurements in this sequence to illustrate the observed hysteresis. Circles: measured data; crosses: experimental points from two to six mirrored to negative bias; dotted line: fit of the low-field part of the data using Eq. (3); solid line: linear fit of the saturated part of the dependence.

in Ref. 4, the soft mode continues to play the key role in the underlying dynamics within our model. We let the high frequency permittivity vary during the fitting procedure although its value is also known quite well ( $\epsilon_\infty \approx 10$ ). This is because of the uncertainty of the absolute value of the experimental permittivity as discussed above. The resulting value of  $\epsilon_\infty$  has, of course, no physical meaning; nevertheless, it can be understood as a quantification of the absolute error of our experimental permittivity (see error bar in Fig. 2).

The bare soft mode frequency obtained from the fits is shown in Fig. 3. One observes that the soft mode exhibits a shift by about  $20 \text{ cm}^{-1}$  for  $90 \text{ kV/cm}$ . Two regimes of the electric field dependence are observed in Fig. 3. For small bias (up to  $\sim 30 \text{ kV/cm}$ ) the field-induced increase in the soft mode frequency is approximately quadratic and can be fitted with Eq. (3); the fit yields  $\beta = 8.5 \times 10^9 \text{ J C}^{-4} \text{ m}^5$ , which is in excellent agreement with the values found in single crystals and unstrained films.<sup>1,3</sup> If the field is further increased a saturated (linear) regime sets in up to  $\sim 100 \text{ kV/cm}$  (above this value the soft mode frequency levels out; data not shown). Switching off the bias field in the linear regime leads to hysteresis effects: the soft mode does not return directly to its zero-field equilibrium state, but it rather follows the straight line of the saturated regime (point 9 in Fig. 3). Then it takes several tens of minutes before it returns into equilibrium or one can apply small negative fields to recover the ground state (point 13 in Fig. 3).

The origin of the central mode that appears in the spectra of many ferroelectric materials in the close vicinity of a displacive-type phase transition is still a subject of scientific debate.<sup>17</sup> There are models assuming its intrinsic origin related to a specific highly anharmonic form of the soft mode potential. The memory effects observed in our work suggest that charged defects play a significant role in the observed tuning: at high fields space-charge regions can be created inside the film, which partially screen the applied bias. The

central mode then could be related to the soft-mode assisted hopping of the charges.

To summarize, we characterized the dielectric properties of STO layers in a strained STO/DSO heterostructure on DSO substrates in the terahertz range. Our results emphasize the key role of the soft mode in the strained films. The existence of the central peak has been previously reported in strained STO films, and frequently it largely dominates the dielectric spectrum; our results provide evidence that the bare central mode is silent and field independent and that its behavior is fully controlled by the soft mode through a strong bilinear coupling. The strained sample shows a significant enhancement in the tunability of both permittivity and losses, which is fully compatible with the deduced soft mode frequency. The structure also shows a potential for applications in the field of modulation of the terahertz light.

The authors wish to thank J. Petzelt for helpful discussions. This work was supported by the Ministry of Education of the Czech Republic (Project No. LC-512) and by the Czech Academy of Sciences (Project No. AVOZ 10100520).

- <sup>1</sup>A. K. Tagantsev, V. O. Sherman, K. F. Astafiev, J. Venkatesh, and N. Setter, *J. Electroceram.* **11**, 5 (2003).
- <sup>2</sup>M. Misra, K. Kotani, I. Kawayama, H. Murakami, and M. Tonouchi, *Appl. Phys. Lett.* **87**, 182909 (2005).
- <sup>3</sup>P. Kužel, F. Kadlec, H. Němec, R. Ott, E. Hollmann, and N. Klein, *Appl. Phys. Lett.* **88**, 102901 (2006).
- <sup>4</sup>P. Kužel, F. Kadlec, J. Petzelt, J. Schubert, and G. Panaitov, *Appl. Phys. Lett.* **91**, 232911 (2007).
- <sup>5</sup>P. A. Fleury and J. M. Worlock, *Phys. Rev.* **174**, 613 (1968).
- <sup>6</sup>P. Kužel and F. Kadlec, *C. R. Phys.* **9**, 197 (2008).
- <sup>7</sup>I. A. Akimov, A. A. Sirenko, A. M. Clark, J.-H. Hao, and X. X. Xi, *Phys. Rev. Lett.* **84**, 4625 (2000).
- <sup>8</sup>J. H. Haeni, P. Irvin, W. Chang, R. Uecker, P. Reiche, Y. L. Li, S. Choudhury, W. Tian, M. E. Hawley, B. Craigo, A. K. Tagantsev, X. Q. Pan, S. K. Streiffner, L. Q. Chen, S. W. Kirchoefer, J. Levy, and D. G. Schlom, *Nature (London)* **430**, 758 (2004).
- <sup>9</sup>W. Chang, J. A. Bellotti, S. W. Kirchoefer, and J. M. Pond, *J. Electroceram.* **17**, 487 (2006); P. Irvin, J. Levy, J. H. Haeni, and D. G. Schlom, *Appl. Phys. Lett.* **88**, 042902 (2006); R. Wördenweber, E. Hollmann, R. Kutzner, and J. Schubert, *J. Appl. Phys.* **102**, 044119 (2007); A. Vasudevarao, A. Kumar, L. Tian, J. H. Haeni, Y. L. Li, C.-J. Eklund, Q. X. Jia, R. Uecker, P. Reiche, K. M. Rabe, L. Q. Chen, D. G. Schlom, and V. Gopalan, *Phys. Rev. Lett.* **97**, 257602 (2006).
- <sup>10</sup>J. Petzelt, P. Kužel, I. Rychetský, A. Pashkin, and T. Ostapchuk, *Ferroelectrics* **288**, 169 (2003).
- <sup>11</sup>L. Duvillaret, F. Garet, and J.-L. Coutaz, *IEEE J. Sel. Top. Quantum Electron.* **2**, 739 (1996).
- <sup>12</sup>L. Beckers, J. Schubert, W. Zander, J. Ziesmann, A. Eckau, P. Leinenbach, and C. Buchal, *J. Appl. Phys.* **83**, 3305 (1998).
- <sup>13</sup>A. Dreyhaupt, S. Winnerl, T. Dekorsy, and M. Helm, *Appl. Phys. Lett.* **86**, 121114 (2005).
- <sup>14</sup>A. Nahata, A. S. Weling, and T. F. Heinz, *Appl. Phys. Lett.* **69**, 2321 (1996).
- <sup>15</sup>E. Buixaderas, S. Kamba, and J. Petzelt, *Ferroelectrics* **308**, 131 (2004).
- <sup>16</sup>R. L. Reese, I. J. Fritz, and H. Z. Cummins, *Phys. Rev. B* **7**, 4165 (1973).
- <sup>17</sup>A. Bussmann-Holder, H. Büttner, and A. R. Bishop, *Phys. Rev. Lett.* **99**, 167603 (2007).